

# TM-PATHVQA: 90000+ Textless Multilingual Questions for Medical Visual Question Answering

Tonmoy Rajkhowa, Amartya Roy Chowdhury, Sankalp Nagaonkar, Achyut Mani Tripathi, S R Mahadeva Prasanna

Indian Institute of Technology, Dharwad, India

212022001@iitdh.ac.in, amartya.chowdhury@iitdh.ac.in, 210020031@iitdh.ac.in,  
t.achyut@iitdh.ac.in, prasanna@iitdh.ac.in

## Abstract

In healthcare and medical diagnostics, Visual Question Answering (VQA) may emerge as a pivotal tool in scenarios where analysis of intricate medical images becomes critical for accurate diagnoses. Current text-based VQA systems limit their utility in scenarios where hands-free interaction and accessibility are crucial while performing tasks. A speech-based VQA system may provide a better means of interaction where information can be accessed while performing tasks simultaneously. To this end, this work implements a speech-based VQA system by introducing a Textless Multilingual Pathological VQA (TM-PathVQA) dataset, an expansion of the PathVQA dataset, containing spoken questions in English, German & French. This dataset comprises 98,397 multilingual spoken questions and answers based on 5,004 pathological images along with 70 hours of audio. Finally, this work benchmarks and compares TM-PathVQA systems implemented using various combinations of acoustic and visual features.

**Index Terms:** Multi-Modal Frameworks, Human-Computer Interaction, Visual Question Answering

## 1. Introduction

In the realm of healthcare and medical diagnostics, Visual Question Answering (VQA) [1, 2] may emerge as a pivotal tool for analyzing complex medical images [3]. It may enable healthcare professionals to inquire about specific details within the visuals, fostering a deeper understanding. VQA may bridge complex medical visuals and human interpretation, thereby improving healthcare diagnosis. However, current VQA systems rely on text-based questions [4, 5], limiting their utility in scenarios where hands-free interaction and accessibility are crucial, particularly in healthcare settings. Hence, integrating speech may enhance the user experience by offering a more natural mode of interaction while performing tasks simultaneously [6, 7, 8, 9]. Thus, a speech-based VQA system would allow for hands-free operation where typing might be cumbersome. Hence, with this motivation, this work proposes a spoken VQA system that can accept multilingual spoken queries. The responses could still be displayed in textual form, enabling better perception and documentation for future references.

The development of a clinically significant spoken VQA system requires training using a dataset comprising spoken questions along with textual answers based on medical images. Without any such existing dataset, the PathVQA dataset [10] is extended by converting the textual questions into spoken form using a Direct Text-to-Speech Translation (DT2ST) [11] system. Subsequently, this resulted in the creation of a Textless Multilingual Pathological Visual Question Answering (TM-PathVQA) dataset, featuring spoken questions in English, Ger-

man and French, tailored for this task. Notably, this paper also implements a Multi-Modal Learning (MML) framework to evaluate the efficacy of TM-PathVQA dataset by addressing the "Yes or No" and open-ended type questions separately. Furthermore, this work also presents a comparative analysis between the frameworks implemented by incorporating various combinations of audio and image features extracted using various state-of-the-art models.

Development of VQA systems for the medical domain began with the introduction of the VQA-Med [12] dataset, which contains medical images and questions that require analysis of both visual content and medical context. VQA-RAD [13] incorporates Radiology reports into the VQA task for medical images. However, these two datasets were domain-specific. This led to the creation of PathVQA [10] covering diverse Pathological contents. Hence, these attributes motivated us to extend the PathVQA to contain spoken questions. To the best of our knowledge, this is the first-ever VQA dataset that incorporates speeches to facilitate the development of a spoken VQA system.

This paper presents three primary contributions. Firstly, it introduces the first-ever TM-PathVQA dataset featuring spoken questions in four languages *viz.* English, German, and French. Secondly, it also introduces a novel framework for implementing TM-PathVQA systems. Finally, this paper presents a diverse set of benchmark evaluations on this dataset by comparing TM-PathVQA systems that were implemented using various audio and image features extracted using various state-of-the-art models. The overview of this paper is as follows: Section 2 provides an overview of the TM-PathVQA dataset and its development process. Section 3 describes the details of different Multimodal Learning Frameworks (MML). Section 4 presents the benchmark results and discussions. Finally, Section 5 concludes the paper and suggests potential directions for future research.

## 2. TM-PathVQA Dataset

The TM-PathVQA dataset is created by extending the PathVQA dataset. PathVQA is recognized as the most extensive dataset developed for pathological VQA tasks. The textual questions in PathVQA were converted into English, German, and French speeches using the SeamlessM4T multimodal and multilingual AI translation model [11]. This resulted in a dataset containing medical visuals paired with spoken questions in three languages *viz.* English, German, and French, alongside answers in English text. This led to the inclusion of  $98,397$  question-answer pairs ( $32,799$  questions for each language  $\times 3 = 98,397$  multilingual questions) derived from 5,004 pathological images along with 70 hours of audio containing spoken questions in those three languages. An illustration in Figure 1 demonstrates a sample

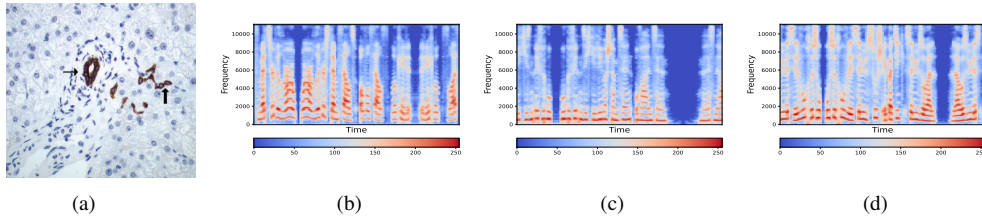


Figure 1: (a) Pathological Image and Spectrogram Visualization of Corresponding Speech-Based Question & Answer in (b) English (Q: "Where are liver stem cells (oval cells) located?", Ans: *In the canals of hering.*), (c) German (Q: "Wo befinden sich Leberstammzellen (ovale Zellen)?", Ans: *In the canals of hering.*) and (d) French (Q: "Où se trouvent les cellules souches hépatiques (cellules ovales)?", Ans: *In the canals of hering.*) Languages from the TM-PathVQA Dataset.

including a medical image and corresponding spectrogram visualizations of English, German, and French questions, along with their answers. Subsequently, the TM-PathVQA dataset is partitioned into the non-overlapping train, validation, and test sets to cover both "Yes / No" and open-ended type questions. A comparative statistical overview of the TM-PathVQA dataset is presented in Table 1, with the final dataset containing 98,397 multilingual question-answer pairs associated with 5,004 medical images.

Table 1: Specification of TM-PathVQA dataset

Set	# of Images	# of QA pairs	Audio duration (in hours)		
			ENGLISH	GERMAN	FRENCH
Train	3,021	19,755	12.87	15.25	13.89
Validation	992	6,279	4.03	4.79	4.34
Test	991	6,761	4.4	5.23	4.75
<b>Total</b>	<b>5,004</b>	<b>32,799</b>	<b>21.3</b>	<b>25.27</b>	<b>22.98</b>

### 3. Experimental Methodology

This section outlines the implementation of TM-PathVQA system in details.

#### 3.1. Representations for Different Modalities

Various types of feature representations that were employed to implement the system are as follows:

##### 3.1.1. Text Representation

The Language-agnostic BERT Sentence Encoder (LaBSE) [14], a BERT-based model [15], was used to generate embeddings from texts. Inspired by the success of LaBSE, this work utilizes its capabilities to extract features from text-based questions.

##### 3.1.2. Audio Representation

Audio features were extracted from the raw spoken questions, sampled at 16 kHz, using Wav2Vec2 [16] (having 1920 dimensions) and Hu-BERT [17] (having 768 dimensions) along with 80-dimensional Mel filterbanks having a window length of 400 and a hop length of 160 frames. For Wav2Vec2 features, the XLS-R 128 [18] pre-trained model was employed. Hu-BERT features were extracted from the 11<sup>th</sup> layer of the encoder and then normalized before feeding into the MML framework. Features were extracted from the last encoder layer using the Whisper large-V3 [19] pre-trained model.

#### 3.1.3. Visual Representation

Image features were extracted using state-of-the-art models, including Vision Transformer (ViT) [20], ResNet-152 [21], VGG19 [22], and Faster-RCNN [23]. ViT divides the image into overlapping patches and feeds them into a Transformer encoder, utilizing the Attention Mechanism [24] to extract image features. Features were extracted from ResNet-152 from its final layer. VGG19, a Convolutional Neural Network (Conv-2D) [25] with 19 layers, employs smaller filters and strides to reduce memory complexity. Features were extracted from the final layer of VGG19 after max-pooling. Faster RCNN, an enhanced version of RCNN [26], is also utilized for feature extraction. Faster-RCNN incorporates a Regional Proposed Network (RPN) [27] on top of the ConvNet-extracted [28] features to generate object proposals. These proposals were then passed to a classification layer to return bounding boxes.

### 3.2. MML Framework for TM-PathVQA

The proposed MML framework comprises three modules: a feature extraction module for processing input images, another module for processing input raw audio signals, and a Transformer [29] encoder responsible for processing these inputs and generating responses. All these modules form the TM-PathVQA architecture. Speech input sequences were down-sampled using a series of stacked 2-dimensional Convolutional (Conv-2D) layers. Each Conv-2D layer had a stride of 4 with 5 channels, resulting in sequence reduction by four times. Then, these audio representations were concatenated with image representations before feeding as input to the Transformer encoder [29].

The encoder comprises two layers of Transformer blocks, each consisting of two Multi-Head Attention [29] with an output dimension of 64. It is then followed by a Multi-Layer Perceptron (MLP) layer with 128 hidden units. The feed-forward block utilizes 256-dimensional inner states, followed by layer-normalization [30]. A dropout [31] rate of 0.2 is applied in the attention block and the MLP layer. The output is then passed to a classification layer represented as  $\hat{y} \in \mathbb{R}^C$ , where  $C$  denotes the number of classes (unique words in the text containing answers). For open-ended questions, the number of classes were 4092, while for "Yes/No" type questions, there were only two classes *i.e.* "Yes" or "No." The final classification is then performed using the Softmax activation function.

The proposed MML TM-PathVQA framework was trained for 100 epochs with a batch size of 64. The model with the lowest validation loss was selected for performance evaluation on the test set. Adam [32] optimizer with a Learning Rate (LR) of  $1 \times 10^{-4}$ , along with the ReduceLROnPlateau [33] scheduler,

Table 2: Performances of English text-based TM-PathVQA systems for Multiclass Classification

Sl. No.	Text Features	Image Features	Performances expressed in %				
			Top-1	Bleu-1	Bleu-2	Bleu-3	F1-score
1	LaBSE	ViT	45.29 ↓ (6.5)	45.53 ↓ (6.84)	2.27 ↓ (1.63)	0.19 ↓ (0.27)	2.24 ↓ (2.14)
2	LaBSE	ResNet-152	43.81 ↓ (7.98)	44.81 ↓ (7.56)	1.93 ↓ (1.97)	0 ↓ (0.46)	1.64 ↓ (2.74)
3	LaBSE	VGG 19	47.69 ↓ (4.1)	48.12 ↓ (4.25)	2.18 ↓ (1.72)	0.16 ↓ (0.3)	3.36 ↓ (1.02)
4	LaBSE	Faster RCNN	<b>51.79</b>	<b>52.37</b>	<b>3.9</b>	<b>0.46</b>	<b>4.38</b>

Table 3: Performances of multilingual speech-based TM-PathVQA systems for Binary Classification using Top-1 accuracy metric (expressed in %)

Sl. No.	Audio Features	Image Features	ENGLISH	GERMAN	FRENCH
1	Wav2Vec2	ViT	52.38 ↓ (4.54)	54.37 ↓ (2.39)	52.37 ↓ (3.99)
2	Wav2Vec2	ResNet-152	53.38 ↓ (3.54)	53.92 ↓ (2.84)	52.92 ↓ (3.44)
3	Wav2Vec2	VGG 19	54.38 ↓ (2.54)	54.38 ↓ (2.38)	52.38 ↓ (3.98)
4	Wav2Vec2	Faster RCNN	<b>56.92</b>	<b>56.76</b>	<b>56.36</b>
5	Hu-BERT	ViT	56.12 ↓ (2.32)	56.22 ↓ (1.09)	55.46 ↓ (1.97)
6	Hu-BERT	ResNet-152	56.26 ↓ (2.18)	56.67 ↓ (0.64)	55.65 ↓ (1.78)
7	Hu-BERT	VGG 19	56.85 ↓ (1.59)	54.78 ↓ (2.53)	55.77 ↓ (1.66)
8	Hu-BERT	Faster RCNN	<b>58.44</b>	<b>57.31</b>	<b>57.43</b>
9	melfilterbank	ViT	53.77 ↓ (3.08)	51.77 ↓ (3.57)	50.23 ↓ (6.04)
10	melfilterbank	ResNet-152	54.53 ↓ (2.32)	53.65 ↓ (1.69)	52.44 ↓ (3.83)
11	melfilterbank	VGG 19	54.73 ↓ (2.12)	50.28 ↓ (5.06)	50.96 ↓ (5.31)
12	melfilterbank	Faster RCNN	<b>56.85</b>	<b>55.34</b>	<b>56.27</b>
13	Whisper	ViT	50.24 ↓ (1.4)	50.67 ↓ (0.87)	50.16 ↓ (1.05)
14	Whisper	ResNet-152	51.28 ↓ (0.36)	50.01 ↓ (1.53)	50.48 ↓ (0.73)
15	Whisper	VGG 19	51.11 ↓ (0.53)	51.03 ↓ (0.51)	50.33 ↓ (0.88)
16	Whisper	Faster RCNN	<b>51.64</b>	<b>51.54</b>	<b>51.21</b>

Table 4: Performances of English text-based TM-PathVQA systems for Binary Classification using Top-1 metric (expressed in %)

Sl. No.	Text Features	Image Features	English
1	LaBSE	ViT	52.73 ↓ (1.65)
2	LaBSE	ResNet-152	49.75 ↓ (4.63)
3	LaBSE	VGG 19	51.66 ↓ (2.75)
4	LaBSE	Faster RCNN	<b>54.38</b>

was employed. A gradient clipping of 0.1 was also applied. All these experiments were conducted using an A100 GPU with 80 gigabytes (GB) of high-bandwidth memory (HBM2e) and Ubuntu 20.04 LTS as the operating system.

### 3.3. Evaluation Metrics

The metric used for binary "Yes/No" type questions is Top-1 [34] accuracy, while for multiclass classification, along with Top-1 accuracy, BLEU-1, BLEU-2, BLEU-3, [35] and F1 [36] accuracy are used. Top-1 Accuracy measures the percentage of questions for which the correct answer is ranked first, providing a straightforward assessment of overall accuracy. BLEU-1, BLEU-2 and BLEU-3 metrics were applied to evaluate answer quality based on n-gram overlap, offering insights into exact and partial matches. F1 score provides a more detailed understanding by considering both false positives and false negatives in handling diverse and open-ended queries about images.

## 4. Results & Discussions

Tables 2, 3, 4 & 5 presents the performance comparison between various MML-based VQA systems. The performance differences against the system that has the best combination are highlighted in blue. From all the tables, Faster RCNN frameworks outperformed other image features for binary and multiclass classification tasks. From Tables 3 & 4, the speech-based VQA systems outperformed their text counterparts for both tasks when the best combinations were considered. For multiclass speech-based systems, all the languages achieved similar performance, with English marginally better. Audio features extracted using Hu-BERT also performed better than other acoustic features. From all these tables, it can be inferred that speech-based TM-PathVQA systems have better potential and utility compared to their text counterparts.

Access to the dataset and corresponding code is provided via the following link: [https://github.com/aquario15/path\\_vqa.git](https://github.com/aquario15/path_vqa.git)

## 5. Conclusion

This paper explored the implementation of a speech-based VQA system by introducing the TM-PathVQA dataset. The contributions of this paper include the creation of the first-ever Textless Multi-lingual Pathological VQA dataset in three diverse languages aimed at advancing multi-lingual VQA modeling research. Additionally, this work established baselines for TM-PathVQA systems implemented using various combinations of audio and image features. Speech-based VQA systems, employing Hu-BERT and Faster RCNN, demonstrated superior performance across the three languages compared to text-based systems. Hence, the proposed TM-PathVQA dataset and the

Table 5: Performance comparison of diverse MML frameworks on TM-PathVQA for multiclass setting across three languages.

ENGLISH							
Sl. No.	Audio Features	Image Features	Top-1 Accuracy	Bleu-1	Bleu-2	Bleu-3	F1-score
1	Wav2Vec2	ViT	45.76 ↓(6.58)	45.95 ↓(7.7)	4.34 ↓(0.33)	0.29 ↓(0.14)	2.58 ↓(2.73)
2	Wav2Vec2	ResNet-152	46.39 ↓(5.95)	47.02 ↓(6.63)	3.3 ↓(1.37)	0.33 ↓(0.1)	4.62 ↓(0.69)
3	Wav2Vec2	VGG 19	47.79 ↓(4.55)	48.05 ↓(5.6)	4.16 ↓(0.51)	0.37 ↓(0.06)	4.36 ↓(0.95)
4	Wav2Vec2	Faster RCNN	<b>52.34</b>	<b>53.65</b>	<b>4.67</b>	<b>0.43</b>	<b>5.31</b>
5	Hu-BERT	ViT	47.96 ↓(5.58)	48.81 ↓(5.13)	3.55 ↓(0.67)	0.31 ↓(0.19)	4.84 ↓(0.38)
6	Hu-BERT	ResNet-152	48.12 ↓(5.42)	48.53 ↓(5.41)	3.71 ↓(0.51)	0.33 ↓(0.17)	3.3 ↓(1.92)
7	Hu-BERT	VGG 19	51.63 ↓(1.91)	52.17 ↓(1.77)	3.36 ↓(0.86)	0.34 ↓(0.16)	4.95 ↓(0.27)
8	Hu-BERT	Faster RCNN	<b>53.54</b>	<b>53.94</b>	<b>4.22</b>	<b>0.5</b>	<b>5.22</b>
9	Mel filterbank	ViT	49.27 ↓(2.89)	50.81 ↓(1.58)	3.44 ↓(0.91)	0.63 ↓(0.04)	3.92 ↓(2.06)
10	Mel filterbank	ResNet-152	46.73 ↓(4.43)	47.97 ↓(4.42)	3.36 ↓(0.99)	0.48 ↓(0.19)	4.5 ↓(1.48)
11	Mel filterbank	VGG 19	49.04 ↓(3.12)	49.79 ↓(2.6)	3.06 ↓(1.29)	<b>0.67</b>	3.5 ↓(2.48)
12	Mel filterbank	Faster RCNN	<b>52.16</b>	<b>52.39</b>	<b>4.35</b>	0.52 ↓(0.15)	<b>5.98</b>
13	Whisper	ViT	48.08 ↓(4.52)	48.74 ↓(6.02)	3.64 ↓(1.35)	0.44 ↓(0.33)	4.54 ↓(0.65)
14	Whisper	ResNet-152	47.94 ↓(4.66)	48.36 ↓(6.4)	3.54 ↓(1.45)	0.44 ↓(0.33)	3.11 ↓(2.08)
15	Whisper	VGG 19	50.58 ↓(2.02)	51.08 ↓(3.68)	3.84 ↓(1.15)	0.51 ↓(0.26)	4.37 ↓(0.32)
16	Whisper	Faster RCNN	<b>52.6</b>	<b>54.76</b>	<b>4.99</b>	<b>0.77</b>	<b>5.19</b>
GERMAN							
Sl. No.	Audio Features	Image Features	Top-1 Accuracy	Bleu-1	Bleu-2	Bleu-3	F1-score
1	Wav2Vec2	ViT	43.11 ↓(5.88)	43.56 ↓(6.74)	3.56 ↓(0.45)	0.32 ↓(0.18)	3.27 ↓(1.34)
2	Wav2Vec2	ResNet-152	42.54 ↓(6.54)	43.12 ↓(7.18)	3.34 ↓(0.67)	0.11 ↓(0.39)	4.11 ↓(0.5)
3	Wav2Vec2	VGG 19	42.22 ↓(6.77)	43.38 ↓(6.92)	3.21 ↓(0.8)	0.4 ↓(0.10)	3.32 ↓(1.29)
4	Wav2Vec2	Faster RCNN	<b>48.99</b>	<b>50.3</b>	<b>4.01</b>	<b>0.5</b>	<b>4.61</b>
5	Hu-BERT	ViT	46.34 ↓(7.98)	46.93 ↓(7.89)	3.04 ↓(1.62)	0.16 ↓(0.57)	3.38 ↓(2.02)
6	Hu-BERT	ResNet-152	46.88 ↓(7.44)	47.18 ↓(7.64)	3.68 ↓(0.98)	0.35 ↓(0.38)	4.96 ↓(0.44)
7	Hu-BERT	VGG 19	50.88 ↓(3.44)	51.92 ↓(2.9)	4.14 ↓(0.52)	<b>0.73</b>	<b>5.4</b>
8	Hu-BERT	Faster RCNN	<b>54.32</b>	<b>54.82</b>	<b>4.66</b>	0.57 ↓(0.16)	4.49 ↓(0.91)
9	Mel filterbank	ViT	45.87 ↓(8.43)	46.56 ↓(8.17)	3.22 ↓(1)	0.09 ↓(0.32)	3.21 ↓(1.93)
10	Mel filterbank	ResNet-152	46.11 ↓(8.19)	46.38 ↓(8.35)	2.28 ↓(1.94)	0.12 ↓(0.29)	4.54 ↓(0.6)
11	Mel filterbank	VGG 19	46.23 ↓(8.07)	46.43 ↓(8.3)	4.11 ↓(0.11)	0.21 ↓(0.2)	4.84 ↓(0.3)
12	Mel filterbank	Faster RCNN	<b>54.3</b>	<b>54.73</b>	<b>4.22</b>	<b>0.41</b>	<b>5.14</b>
13	Whisper	ViT	46.46 ↓(1.65)	46.76 ↓(1.87)	4.16 ↓(0.54)	0.19 ↓(0.15)	4.22 ↓(1.01)
14	Whisper	ResNet-152	46.46 ↓(1.65)	46.88 ↓(1.75)	4.02 ↓(0.68)	0 ↓(0.34)	4.17 ↓(1.06)
15	Whisper	VGG 19	44.78 ↓(3.33)	45.27 ↓(3.36)	4.44 ↓(0.26)	0 ↓(0.34)	4.2 ↓(1.03)
16	Whisper	Faster RCNN	<b>48.11</b>	<b>48.63</b>	<b>4.7</b>	<b>0.34</b>	<b>5.23</b>
FRENCH							
Sl. No.	Audio Features	Image Features	Top-1 Accuracy	Bleu-1	Bleu-2	Bleu-3	F1-score
1	Wav2Vec2	ViT	43.31 ↓(5.24)	43.51 ↓(5.38)	4.8 ↓(0.09)	0.19 ↓(0.06)	4.8 ↓(0.4)
2	Wav2Vec2	ResNet-152	42.39 ↓(6.16)	43.89 ↓(5)	4.05 ↓(0.84)	0.12 ↓(0.13)	4.81 ↓(0.39)
3	Wav2Vec2	VGG 19	42.46 ↓(6.09)	43.76 ↓(5.13)	4.66 ↓(0.23)	0.13 ↓(0.12)	4.4 ↓(0.8)
4	Wav2Vec2	Faster RCNN	<b>48.55</b>	<b>48.89</b>	<b>4.89</b>	<b>0.25</b>	<b>5.2</b>
5	Hu-BERT	ViT	47.03 ↓(6.44)	48.22 ↓(5.56)	4.86 ↓(0.1)	0.42 ↓(0.61)	4.85 ↓(1.04)
6	Hu-BERT	ResNet-152	47.98 ↓(5.49)	48.06 ↓(5.72)	4.87 ↓(0.09)	0.48 ↓(0.55)	3 ↓(2.89)
7	Hu-BERT	VGG 19	51.66 ↓(1.81)	52.14 ↓(1.64)	4.77 ↓(0.19)	0.54 ↓(0.49)	4.65 ↓(1.24)
8	Hu-BERT	Faster RCNN	<b>53.47</b>	<b>53.78</b>	<b>4.96</b>	<b>1.03</b>	<b>5.89</b>
9	Mel filterbank	ViT	46.37 ↓(5.37)	46.82 ↓(6.37)	4.07 ↓(0.36)	0.46 ↓(0.15)	4.68 ↓(0.92)
10	Mel filterbank	ResNet-152	48.11 ↓(3.63)	48.33 ↓(9.86)	3.7 ↓(1.73)	<b>0.61</b>	4.96 ↓(0.64)
11	Mel filterbank	VGG 19	47.65 ↓(4.09)	48.68 ↓(4.51)	<b>4.43</b>	0.39 ↓(0.22)	4.73 ↓(0.87)
12	Mel filterbank	Faster RCNN	<b>51.74</b>	<b>53.19</b>	4.04 ↓(0.39)	0.46 ↓(0.15)	<b>5.6</b>
13	Whisper	ViT	47.16 ↓(2.95)	47.96 ↓(2.93)	4.76 ↓(0.01)	<b>0.4</b>	4.16 ↓(0.45)
14	Whisper	ResNet-152	47 ↓(3.11)	47.4 ↓(3.49)	4.23 ↓(0.53)	0.19 ↓(0.21)	4.4 ↓(0.21)
15	Whisper	VGG 19	<b>50.11</b>	<b>50.89</b>	<b>4.77</b>	0.21 ↓(0.19)	4.21 ↓(0.4)
16	Whisper	Faster RCNN	46.91 ↓(3.2)	47.28 ↓(3.61)	4.19 ↓(0.58)	0.36 ↓(0.04)	<b>4.61</b>

experimental benchmarks presented in this study may serve as valuable insights for future research in spoken VQA. Future endeavors will focus on designing novel attention-based MML frameworks that may perform better than the baseline MML frameworks presented in this paper.

## 6. References

- [1] H. Fang, S. Gupta, F. Iandola, R. K. Srivastava, L. Deng, P. Dollár, J. Gao, X. He, M. Mitchell, J. C. Platt *et al.*, "From captions to visual concepts and back," in *Proceedings of the IEEE conference on computer vision and pattern recognition*, 2015, pp. 1473–

- [2] X. Chen and C. L. Zitnick, "Learning a recurrent visual representation for image caption generation," *arXiv preprint arXiv:1411.5654*, 2014.
- [3] M. Kachuee, S. Fazeli, and M. Sarrafzadeh, "Ecg heartbeat classification: A deep transferable representation," in *2018 IEEE International Conference on Healthcare Informatics (ICHI)*, 2018, pp. 443–444.
- [4] S. Antol, A. Agrawal, J. Lu, M. Mitchell, D. Batra, C. L. Zitnick, and D. Parikh, "Vqa: Visual question answering," in *Proceedings of the IEEE International Conference on Computer Vision (ICCV)*, December 2015.
- [5] P. Anderson, X. He, C. Buehler, D. Teney, M. Johnson, S. Gould, and L. Zhang, "Bottom-up and top-down attention for image captioning and visual question answering," in *2018 IEEE/CVF Conference on Computer Vision and Pattern Recognition*, 2018, pp. 6077–6086.
- [6] T. Zhang, D. Dai, T. Tuytelaars, M.-F. Moens, and L. Van Gool, "Speech-based visual question answering," *arXiv preprint arXiv:1705.00464*, 2017.
- [7] A. P. Patil, A. Behera, P. Anusha, M. Seth, and Prabhuling, "Speech enabled visual question answering using lstm and cnn with real time image capturing for assisting the visually impaired," in *TENCON 2019 - 2019 IEEE Region 10 Conference (TENCON)*, 2019, pp. 2475–2480.
- [8] F. Alasmay and S. Al-Ahmadi, "Sbvqa 2.0: Robust end-to-end speech-based visual question answering for open-ended questions," *IEEE Access*, vol. 11, pp. 140 967–140 980, 2023.
- [9] I. Chowdhury, K. Nguyen, C. Fookes, and S. Sridharan, "A cascaded long short-term memory (lstm) driven generic visual question answering (vqa)," in *2017 IEEE International Conference on Image Processing (ICIP)*, 2017, pp. 1842–1846.
- [10] X. He, Y. Zhang, L. Mou, E. Xing, and P. Xie, "Pathvqa: 30000+ questions for medical visual question answering," *arXiv preprint arXiv:2003.10286*, 2020.
- [11] L. Barrault, Y.-A. Chung, M. C. Meglioli, D. Dale, N. Dong, P.-A. Duquenne, H. Elshahar, H. Gong, K. Heffernan, J. Hoffman *et al.*, "Seamless4t-massively multilingual & multimodal machine translation," *arXiv preprint arXiv:2308.11596*, 2023.
- [12] A. Ben Abacha, M. Sarrouiti, D. Demner-Fushman, S. A. Hasan, and H. Müller, "Overview of the vqa-med task at imageclef 2021: Visual question answering and generation in the medical domain," in *CLEF 2021 Working Notes*, ser. CEUR Workshop Proceedings. Bucharest, Romania: CEUR-WS.org, September 21–24 2021.
- [13] L.-M. Zhan, B. Liu, L. Fan, J. Chen, and X.-M. Wu, "Medical visual question answering via conditional reasoning," in *Proceedings of the 28th ACM International Conference on Multimedia*, 2020, pp. 2345–2354.
- [14] F. Feng, Y. Yang, D. Cer, N. Arivazhagan, and W. Wang, "Language-agnostic bert sentence embedding," *arXiv preprint arXiv:2007.01852*, 2020.
- [15] J. Devlin, M.-W. Chang, K. Lee, and K. Toutanova, "Bert: Pre-training of deep bidirectional transformers for language understanding," *arXiv preprint arXiv:1810.04805*, 2018.
- [16] A. Baevski, Y. Zhou, A. Mohamed, and M. Auli, "wav2vec 2.0: A framework for self-supervised learning of speech representations," *Advances in neural information processing systems*, vol. 33, pp. 12 449–12 460, 2020.
- [17] W.-N. Hsu, B. Bolte, Y.-H. H. Tsai, K. Lakhota, R. Salakhutdinov, and A. Mohamed, "Hubert: Self-supervised speech representation learning by masked prediction of hidden units," *IEEE/ACM Transactions on Audio, Speech, and Language Processing*, vol. 29, pp. 3451–3460, 2021.
- [18] A. Babu, C. Wang, A. Tjandra, K. Lakhota, Q. Xu, N. Goyal, K. Singh, P. von Platen, Y. Saraf, J. Pino *et al.*, "Xls-r: Self-supervised cross-lingual speech representation learning at scale," *arXiv preprint arXiv:2111.09296*, 2021.
- [19] A. Radford, J. W. Kim, T. Xu, G. Brockman, C. McLeavey, and I. Sutskever, "Robust speech recognition via large-scale weak supervision," in *International Conference on Machine Learning*. PMLR, 2023, pp. 28 492–28 518.
- [20] A. Dosovitskiy, L. Beyer, A. Kolesnikov, D. Weissenborn, X. Zhai, T. Unterthiner, M. Dehghani, M. Minderer, G. Heigold, S. Gelly *et al.*, "An image is worth 16x16 words: Transformers for image recognition at scale," *arXiv preprint arXiv:2010.11929*, 2020.
- [21] K. He, X. Zhang, S. Ren, and J. Sun, "Deep residual learning for image recognition," in *Proceedings of the IEEE conference on computer vision and pattern recognition*, 2016, pp. 770–778.
- [22] K. Simonyan and A. Zisserman, "Very deep convolutional networks for large-scale image recognition," *arXiv preprint arXiv:1409.1556*, 2014.
- [23] S. Ren, K. He, R. Girshick, and J. Sun, "Faster r-cnn: Towards real-time object detection with region proposal networks," *Advances in neural information processing systems*, vol. 28, 2015.
- [24] J. Wang and S. Li, "Self-attention mechanism based system for dcase2018 challenge task1 and task4," *Proc. DCASE Challenge*, pp. 1–5, 2018.
- [25] C. Cheng and K. K. Parhi, "Fast 2d convolution algorithms for convolutional neural networks," *IEEE Transactions on Circuits and Systems I: Regular Papers*, vol. 67, no. 5, pp. 1678–1691, 2020.
- [26] K. He, G. Gkioxari, P. Dollár, and R. Girshick, "Mask r-cnn," in *Proceedings of the IEEE international conference on computer vision*, 2017, pp. 2961–2969.
- [27] Y. Ye, H. Chen, C. Zhang, X. Hao, and Z. Zhang, "Sarpnet: Shape attention regional proposal network for lidar-based 3d object detection," *Neurocomputing*, vol. 379, pp. 53–63, 2020.
- [28] D. Tran, J. Ray, Z. Shou, S.-F. Chang, and M. Paluri, "Convnet architecture search for spatiotemporal feature learning," *arXiv preprint arXiv:1708.05038*, 2017.
- [29] A. Vaswani, N. Shazeer, N. Parmar, J. Uszkoreit, L. Jones, A. N. Gomez, L. u. Kaiser, and I. Polosukhin, "Attention is all you need," in *Advances in Neural Information Processing Systems*, I. Guyon, U. V. Luxburg, S. Bengio, H. Wallach, R. Fergus, S. Vishwanathan, and R. Garnett, Eds., vol. 30. Curran Associates, Inc., 2017.
- [30] J. L. Ba, J. R. Kiros, and G. E. Hinton, "Layer normalization," *arXiv preprint arXiv:1607.06450*, 2016.
- [31] N. Srivastava, "Improving neural networks with dropout," *University of Toronto*, vol. 182, no. 566, p. 7, 2013.
- [32] D. P. Kingma and J. Ba, "Adam: A method for stochastic optimization," *arXiv preprint arXiv:1412.6980*, 2014.
- [33] A. Al-Kababji, F. Bensaali, and S. P. Dakua, "Scheduling techniques for liver segmentation: Reducelronplateau vs onecyclelr," in *International Conference on Intelligent Systems and Pattern Recognition*. Springer, 2022, pp. 204–212.
- [34] S. Niu, J. Guo, Y. Lan, and X. Cheng, "Top-k learning to rank: labeling, ranking and evaluation," in *Proceedings of the 35th international ACM SIGIR conference on Research and development in information retrieval*, 2012, pp. 751–760.
- [35] K. Papineni, S. Roukos, T. Ward, and W.-J. Zhu, "Bleu: a method for automatic evaluation of machine translation," ser. ACL '02. USA: Association for Computational Linguistics, 2002, p. 311–318.
- [36] R. Yacouby and D. Axman, "Probabilistic extension of precision, recall, and f1 score for more thorough evaluation of classification models," in *Proceedings of the first workshop on evaluation and comparison of NLP systems*, 2020, pp. 79–91.